UDC669.14:621.74.047-837

Advances of Applied MHD Technology for Continuous Casting Process

Eiichi Takeuchi*1
Hiroshi Harada*1
Hiroyuki Tanaka*1
Takanobu Ishii*2
Takehiko Toh*1
Masafumi Zeze*1
Masatake Hojo*1
Kiyoshi Shigematsu*3

Abstract:

The continuous casting process is near perfection in terms of productivity and quality. For its further advance from the viewpoint of both economy and technology so that it may prove a truly viable production process toward the coming century, attention is now focused on the applied MHD technology. A typical example of Nippon Steel's applied MHD technology is the control of molten steel flow in the mold by electromagnetic stirring and braking. In this paper, features of these flow control techniques are described from a MHD point of view. In particular, simulation experiment and numerical analysis clarify the interference between the steel flow as discharged from the immersion nozzle and that as driven by electromagnetic force, as well as the relationship between the flow field and the electromagnetic field that changes with electric boundary conditions. Also introduced are some of the characteristic metallurgical benefits of electromagnetic stirring and braking confirmed by plant tests. Further, description is made of the technique of controlling the initial solidification of steel in the mold by an alternating-current magnetic field that has been attracting increasing attention in recent years, according to the results of simulation test and steel casting test.

1. Introduction

In the past decade, the continuous casting process has markedly progressed, solved many technological problems, and widely spread as a result. In the meantime, attempts have been made at developing novel casting processes for further innovation toward the coming century. Among them, application of magnetohydrodynamics (MHD) has aroused a great deal of interest as powerful elementary technology to develop casting processes with higher productivity and better cast steel quality.

Nippon Steel started the application of MHD with the develop-

*1 Technology Development Bureau
*2 Nagoya Works
*3 Oita Works

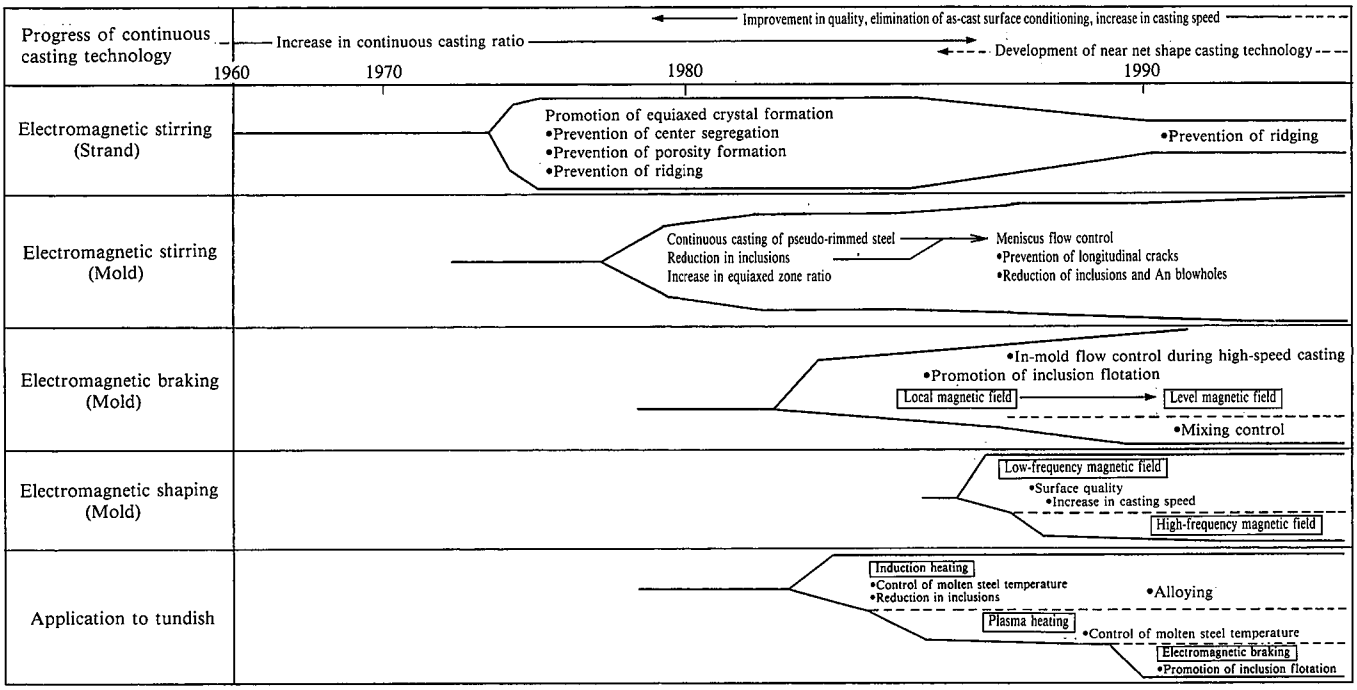

Fig. 1 Changes in applied MHD techniques for continuous casting process

ment of a strand pool electromagnetic stirrer in the middle of 1960 for the purpose of improving the internal quality of the cast steel, as shown in **Fig. 1**. The equipment, which has the merit of raising the equiaxed zone ratio, was installed on various continuous casters to prevent center segregation, porosity, and ridging in the late 1970s. The 1980s saw the development of in-mold electromagnetic stirring for continuously casting pseudo-rimmed steel, a grade then still to be brought under continuous casting. The in-mold electromagnetic stirring technique has proved effective in suppressing the formation of CO bubbles as originally planned as well as in preventing longitudinal surface cracks and reducing subsurface inclusions. It is now extensively utilized to improve the surface quality of cast steel. In the late 1980s, in-mold electromagnetic braking drew attention as a useful technique for high-speed casting. Nippon Steel worked on the development of a new type of electromagnetic braking technique that uniformly applies a direct-current (DC) magnetic field across the width of the strand being cast. This resulted in solving the problem of stabilizing the metallurgical effect of conventional localized electromagnetic braking, and also in discovering a new function of preventing the molten steel in the upper strand pool from mixing with that in the lower strand pool. This new in-mold electromagnetic brake of the uniform DC magnetic field type is finding increasing usage.

This paper clarifies the characteristics of MHD phenomena as the bases of the in-mold electromagnetic stirrer and the electromagnetic brake of the level DC magnetic field type, and describes the effects of the MHD phenomena on the metallurgical phenomena of continuous casting. The technique of controlling the initial solidification of continuously cast steel by utilizing electromagnetic pressure has been a subject of on-going research and development in recent years. The results of verification of the technique by plant tests are introduced. Reference is made also to the future prospect of applied MHD technology for the continuous casting process.

2. In-mold Electromagnetic Stirring by Traveling Magnetic Field

The in-mold electromagnetic stirrer is schematically illustrated in **Fig. 2**. A linear motor is installed in the upper part of the water box in the wide face of the mold. The linear motor horizontally recirculates the molten steel near the meniscus by generating a traveling magnetic field that covers the full width of the mold[1]. Several new techniques are incorporated to enhance the electromagnetic stirring efficiency. For example, the attenuation of magnetic flux density is minimized by using stainless steel-clad copper plates or light-gage copper plates of low electrical conductivity, and adopting a 10 Hz or lower-frequency traveling magnetic field. Low-melting-point alloy experimentation and numerical analysis showed that the distance between the linear motor and the meniscus has a great effect on the meniscus flow velocity and flow pattern. Necessary equipment measures were taken accordingly.

2.1 Numerical simulation of flow in mold

A magnetic field traveling through a molten steel pool induces

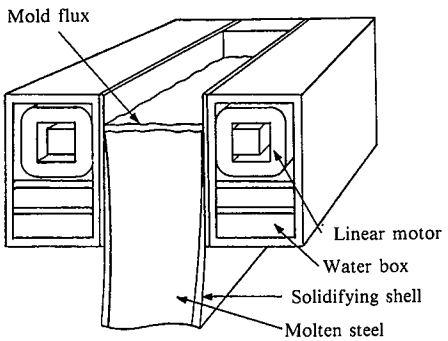

Fig. 2 Schematic illustration of in-mold electromagnetic stirrer

electric current in the molten steel. The interaction of the traveling magnetic field and the induced current produces the Lorentz force, which in turn drives the molten steel. The induced current path is greatly affected by the surrounding electric boundary conditions, and the electromagnetic force does not necessarily have a component in the mold width direction alone. The discharge stream from the immersion nozzle causes the flow of molten steel in the mold. This flow interferes with the flow driven by the linear motor.

Prediction of the flow field is indispensable for efficiently exploiting the metallurgical benefits of in-mold electromagnetic stirring in this complex system. The behavior of molten metal in an electromagnetic field can be numerically determined by coupling Maxwell's equations [Eqs. (1) to (3)][2], Ohm's law [Eq. (4)], and the equation of continuity [Eq. (5)] and Navier-Stokes equation [Eq. (6)] for incompressible fluids.

$$\nabla \times \mathbb{E} = -\partial \mathbb{B}/\partial t \quad \cdots\cdots(1)$$

$$\nabla \times \mathbb{B} = \mu \mathbb{J} \quad \cdots\cdots(2)$$

$$\nabla \cdot \mathbb{B} = 0 \quad \cdots\cdots(3)$$

$$\mathbb{J} = \sigma(\mathbb{E} + \mathbb{U} \times \mathbb{B}) \quad \cdots\cdots(4)$$

$$\nabla \cdot \mathbb{U} = 0 \quad \cdots\cdots(5)$$

$$\rho\{\partial \mathbb{U}/\partial t + (\mathbb{U} \cdot \nabla)\mathbb{U}\} = -\nabla P + \nu\rho\nabla^2\mathbb{U} + \rho g + \mathbb{J} \times \mathbb{B} \quad \cdots\cdots(6)$$

Figs. 3 and **4** show the effect of the nozzle port angle on the in-mold electromagnetic stirring-driven flow as typical results of analysis. As numerical analysis techniques, the finite element method and the large eddy simulation (LES)/finite difference method were used for analyzing the magnetic field and the flow field, respectively. The mold width and thickness were 1,830 and 280 mm, respectively, and the casting speed was 1.3 m/min. **Figs. 3**(a) and (b) show the flow velocity distributions in the mold meniscus position on the transverse section and in the solidifying shell front position on the longitudinal section without and with in-mold electromagnetic stirring, respectively, when the nozzle port angle was 15°. Without in-mold electromagnetic stirring, the stream discharged from the nozzle port impinges on the narrow face of the mold, reverses in direction, turns upward, and flows from the meniscus toward the center of the mold **[Fig. 3**(a)]. When electromagnetic stirring is conducted according to this flow pattern, the molten steel is accelerated where the reverse flow and the Lorentz force are in the same direction, and is decelerated where the reverse flow and the Lorentz force are in opposite directions. As a result, a uniform rotating flow pattern cannot always be obtained at the meniscus in the circumferential direction of the strand **[Fig. 3**(b)]. When the nozzle port angle is increased to 35°, the reverse flow does not easily appear at the meniscus **[Fig. 4**(a)], with the result that the flow driven by electromagnetic stirring is not affected by the reverse flow and that a relatively uniform rotating flow is formed **[Fig. 4**(b)].

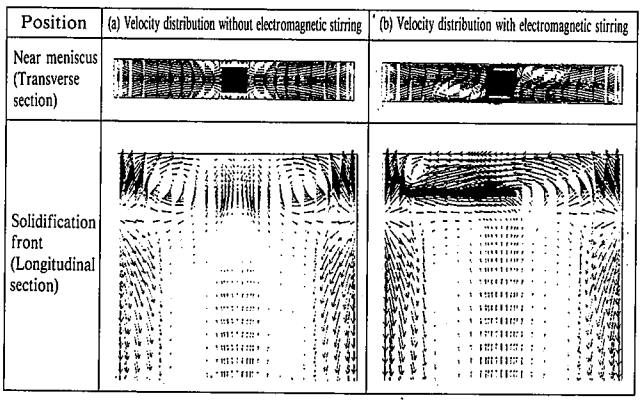

Fig. 3 Effect of nozzle discharge stream ($\theta = 15°$) on molten steel flow with in-mold electromagnetic stirring

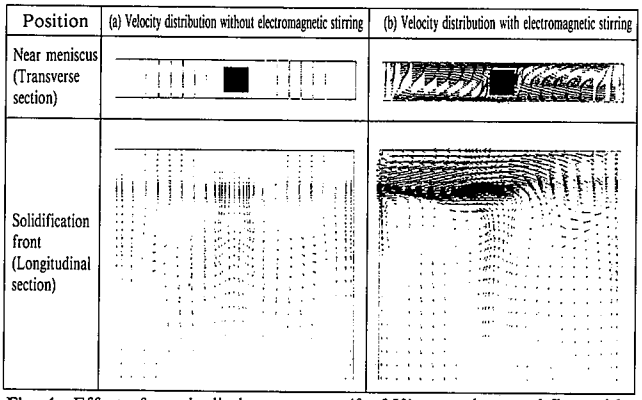

Fig. 4 Effect of nozzle discharge stream ($\theta = 35°$) on molten steel flow with in-mold electromagnetic stirring

When the flow pattern on the solidifying shell along the wide face of the mold is macroscopically examined, it is evident that the stagnant zone between the nozzle and the solidifying shell is eliminated by applying electromagnetic force.

2.2 Effect of in-mold electromagnetic stirring on slab quality

2.2.1 Suppression of CO blowholes during continuous casting of pseudo-rimmed steel

The nozzle port angle and the electromagnetic stirring thrust were selected to obtain a uniform rotating flow pattern at a given velocity near the meniscus in the mold. Pseudo-rimmed steel was continuously cast under the conditions given in **Table 1**.

The formation of CO blowholes during casting can be suppressed by causing the molten steel to flow at the solidification front[1]. As shown in **Fig. 5**, the critical free oxygen concentration of molten steel at which CO blowholes evolve tends to increase with increasing rotating flow velocity at the meniscus. This is because the concentration of solute elements at the solidification front is reduced by the flow, which in turn retards the CO blowhole formation reaction at the solidification front.

2.2.2 Prevention of entrapment of inclusions in slab surface layer

When in-mold electromagnetic stirring was applied to the continuous casting of aluminum-killed sheet steel, it sharply reduced the amount of alumina inclusions within 10 mm of the slab surface[3]. As shown in **Fig. 6**, this effect is outstanding at the midwidth of the slab. This area is where reverse flow patterns collide against each other to cause stagnancy when no electromagnetic force is applied to the molten steel in the mold. Some alumina clusters were probably washed away by the flow generated

Table 1 Casting conditions for pseudo-rimmed steel with in-mold electromagnetic stirring

Steel grade	Low-carbon pseudo-rimmed steel
Casting temperature	1,562 ± 12°C (in tundish)
Casting speed	0.06-1.10 m/min
Mold shape	1,120-2,100 mm wide × 250 mm thick
Meniscus-to-core distance	50 ± 10 mm
Maximum magnetic flux density	0.048 T

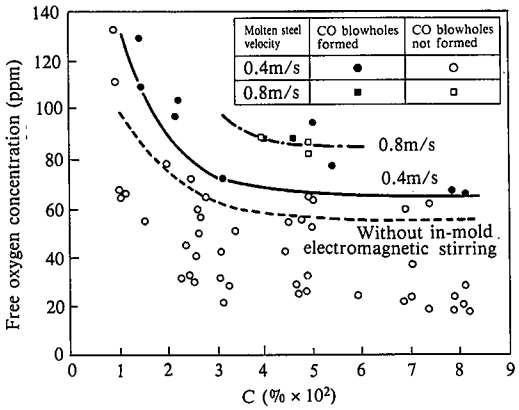

Fig. 5 Suppression of CO blowhole formation by in-mold electromagnetic stirring

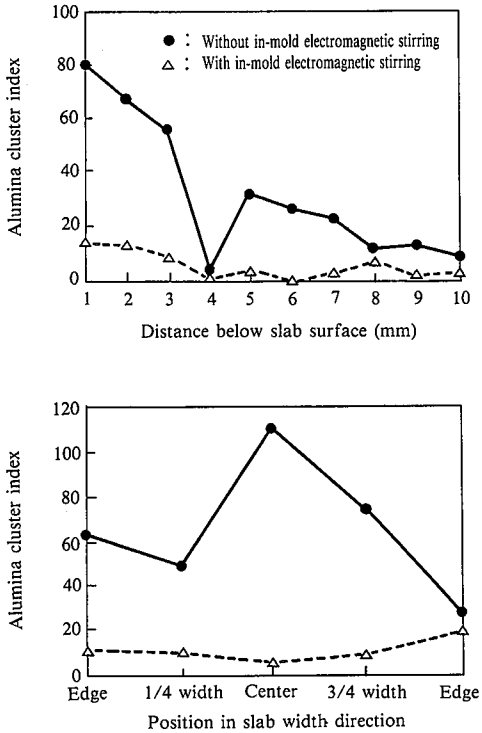

Fig. 6 Reduction in slab subsurface inclusions by in-mold electromagnetic stirring

by the electromagnetic force between the nozzle and the solidifying shell.

2.2.3 Prevention of longitudinal cracks

Fig. 7 shows the way the incidence of longitudinal cracks on the slab surface is reduced when the in-mold electromagnetic stirrer causes the molten steel to flow at the front of the solidifying shell in the initial stage of solidification during the continuous casting of medium-carbon steel[4]. The reduction of longitudinal surface cracks is attributable to the washing action of the electromagnetically stirred flow of molten steel. The washing action should level the shell thickness and reduce the interdendritic segregation.

2.2.4 Reduction in oscillation mark depth

Fig. 8 shows the change of slab surface oscillation mark depth

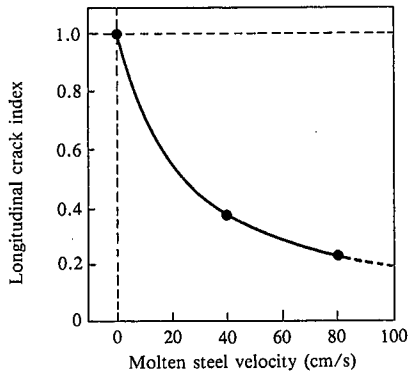

Fig. 7 Reduction in longitudinal crack formation on slab surface by in-mold electromagnetic stirring

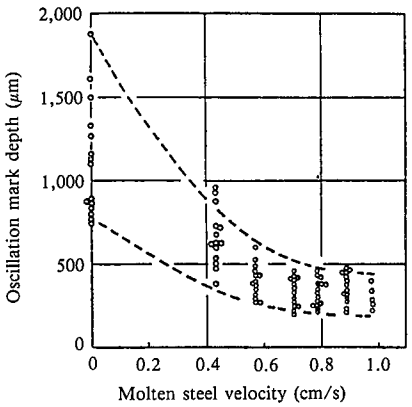

Fig. 8 Reduction in oscillation mark depth by in-mold electromagnetic stirring

with the electromagnetically induced flow of molten steel[1]. As seen, increasing the flow velocity decreases the oscillation mark depth with reduced variability of the mark depth. This phenomenon may be explained as follows. The electromagnetic stirring-induced flow pattern raised and homogenized the meniscus temperature, retarded the growth of initial solidifying shell, reduced the viscosity of the mold powder, and lowered the dynamic pressure of the powder entering the tip of the solidifying shell accompanying the mold oscillation. This explanation may be validated by such phenomena as an increase of about 20% in powder consumption and decrease in hook length of mark subsurface structure as a result of in-mold electromagnetic stirring.

3. Control of Molten Steel Flow in Mold by Level DC Magnetic Field

As a typical example of DC magnetic field application, in-mold electromagnetic braking is being tried by various steelmakers. The in-mold electromagnetic braking technique started as a localized MHD application[5] to directly brake the molten steel stream discharged from the immersion nozzle. At that time, however, the technique had several problems concerning the stability of braking effect and resultant metallurgical benefits. Nippon Steel developed the technique[6, 7] of stably controlling the molten steel flow in the mold by applying a level DC magnetic field across the mold width, and discovered a new function[8] of suppressing mixing in addition to the conventional functions to ensure the slab quality.

3.1 Simulation of in-mold molten steel flow control by level electromagnetic brake

3.1.1 Mercury model experiment

The apparatus used in the experiment is schematically illustrated in **Fig. 9**. It consists of a stainless steel mercury pool vessel, a tundish, and a DC magnet. The vessel measures 100 mm thick, 600 mm wide and 1,500 mm high. It can circulate mercury at such a rate as to be equivalent to the desired casting speed while keeping the meniscus level constant by U-shaped tube construction. The magnetic field is applied to cross the strand thickness. The magnetic flux density is not uniformly distributed in the vertical direction, but is in the transverse direction. The maximum magnetic flux density is 0.55 T at the pole center position.

The position of the electromagnet can be changed in the height direction of the pool. The experiment was conducted in two cases: Case I when the pole center was located 290 mm below the meniscus and Case II when the pole center was located 135 mm below the meniscus. The velocity distribution in the mercury pool was measured for the two cases. Case I corresponds to the condition in which the center of the magnetic field is located below the position where the nozzle discharge stream impinges on the narrow face of the mold. Case II corresponds to the condition in which the magnetic field is set just below the nozzle port. The experimental conditions were established so that similarity between the mercury model and the real continuous cater can be maintained by the Froude number and Stuart number. The velocity in the mercury pool was measured by a Vives sensor.

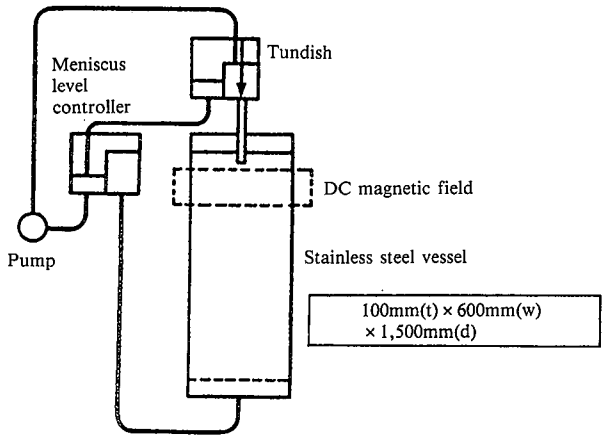

Fig. 9 Schematic diagram of mercury model experimental apparatus

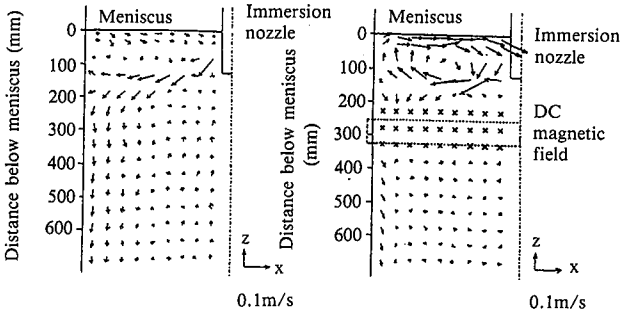

Fig. 10 Simulation of fluid flow control by level magnetic field brake in mercury model experiment (Case I)

Fig. 10 shows the velocity distribution measured in Case I. Without a magnetic field, the nozzle discharge stream impinges on the narrow face of the mold and divides into upward and downward components. The downward flow penetrates deep into the pool and rises at the center of the pool, forming a circulating flow pattern. The upward flow reaches the meniscus and comes back from the narrow face toward the nozzle. When a 0.35 T magnetic field is applied, the circulating flow below the magnetic field is retarded, while the meniscus velocity is accelerated. The velocity was not measured at the X points because the external magnetic field strength was large enough to cause an accuracy problem there. **Fig. 11** shows the change of downward flow velocity with the magnetic flux density at 20 mm from the narrow face of the pool and 630 mm from the meniscus. The downward flow is normalized by the casting speed, and is a plug flow when its velocity is 1. The narrow-face downward flow velocity decays little under the conditions of Case I. Under the conditions of Case II, the downward flow velocity is steeply reduced at 0.3 T and above, and becomes a plug-like flow at 0.55 T.

The application of a level magnetic field can suppress the circulating flow pattern below the magnetic field zone. At the same time, the positional relationship between the level magnetic field and the nozzle port can be judiciously selected to stir the meniscus or obtain a uniform downward flow pattern.

3.1.2 Numerical simulation

When an external DC magnetic field is applied to a moving electrically conductive fluid, electric current is induced in the fluid. The current flowing through the fluid establishes a circuit to meet the law of conservation of electric current, according to the electric boundary conditions, velocity distribution, and magnetic field intensity distribution of the system concerned. Induced current components that cross the external magnetic field at right angles act as electromagnetic braking forces on the fluid. The current path formed in this way contains components in the direction opposite to the braking direction. The actual electromagnetic braking phenomenon is not simple. Hence, substantial understanding of the electromagnetic braking mechanism is indispensable for controlling the flow of molten steel by an electromag-

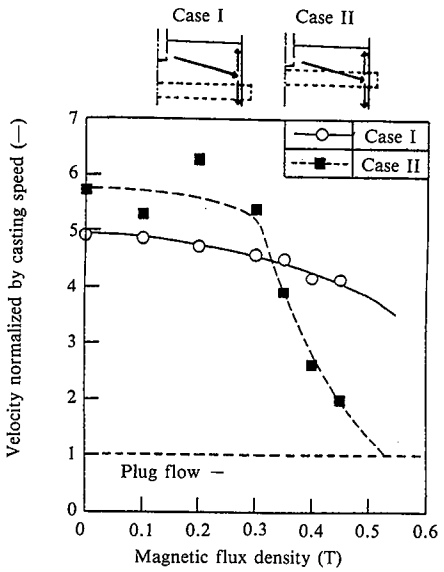

Fig. 11 Effect of magnetic flux density on downward flow velocity (mercury model experiment)

netic brake in such a complex system as the molten steel pool in the mold of a continuous caster.

Concerning the electromagnetic field, Eq. (7) was derived from Maxwell's equations [Eqs. (1) to (3)], Ohm's law [Eq. (4)], and the equation of continuity of electric current[9]. The electric potential density distribution was obtained from Eq. (7) and used to calculate the Lorentz force.

$$\nabla\cdot(\sigma\nabla\phi)=\nabla\cdot\{\sigma(\mathbb{U}\times\mathbb{B})\} \quad \cdots\cdots(7)$$

The k-ε model was used as the turbulence model. As electric boundary condition, the stainless steel plate of the pool vessel was taken as solidifying shell. As inlet boundary conditions, a fully developed turbulent flow was given in the upper part of the nozzle tube, and a free jet was formed at the nozzle port. A wall function that follows the logarithmic law was used as boundary condition in front of the nozzle wall and vessel wall. The effect of the free surface was not taken into account.

Figs. 12(a) and (b) show the calculated velocity distributions when a 0.35 T DC magnetic field was applied under the conditions of Cases I and II, respectively. The velocity of the stream moving down the narrow face in Case II is lower than in Case I, and the downward flow is almost a plug flow. These calculated results agree well with the values observed in the mercury model experiment.

Figs. 13(a) and (b) show the calculated density distributions

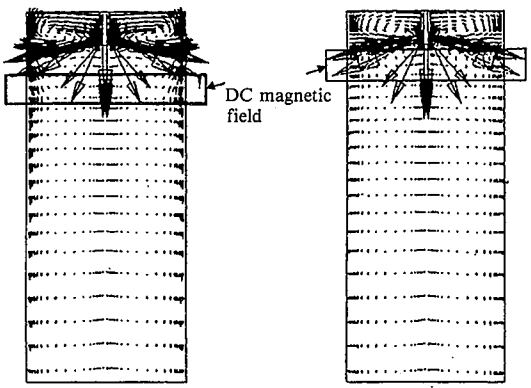

(a) 0.35 T/Case I (b) 0.35 T/Case II

Fig. 12 Results of numerical simulation concerning change in in-mold velocity distribution with level magnetic field brake

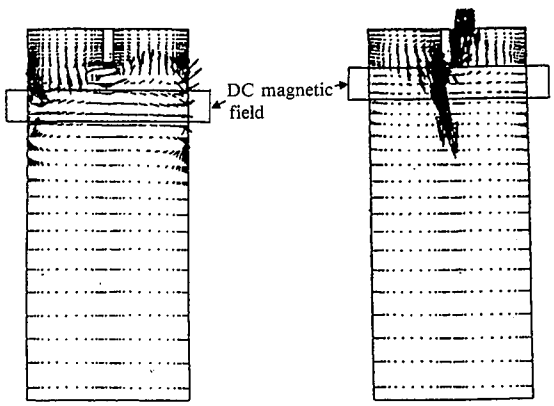

(a) 0.35 T/Case I (b) 0.35 T/Case II

Fig. 13 Effect of electromagnetic brake location on induced current density distribution (results of numerical analysis)

of electric current induced in the molten metal in the pool in Cases I and II, respectively. Under the conditions of Case I, the nozzle discharge stream impinges on the narrow face of the pool, and its downward component crosses the magnetic field zone. Positive and negative electric potential peaks are formed on both narrow faces of the pool, and a horizontal electric current circuit is established in the pool. As a result, an electromagnetic force acts to retard the downward penetration of the nozzle discharge stream and restrict the formation of a circulating flow pattern below the magnetic field zone. Since the direction of the electric current three-dimensionally changes on both narrow faces of the pool where the electric potential peaks exist, the electromagnetic force to brake the downward flow weakens. This results in reducing the breaking effect on the downward flow near the narrow face of the pool. Under the conditions of Case II, the nozzle discharge stream directly crosses the magnetic field zone, so that the electric boundary conditions cause no constraint on the formation of electric current loop. The electric current loop thus formed effectively brakes the nozzle discharge stream, decelerates the downward flow near the narrow face of the pool, and thus accelerates the plug flow tendency.

3.2 Effect of level magnetic field brake on slab quality

3.2.1 Reduction in penetration depth of discharge stream

When molten steel was continuously cast on a 1-ton test machine, a level magnetic field brake was operated below the mold of the caster, and the metallurgical benefits of this molten steel flow control were investigated. Under the casting conditions of **Table 2**(a), a sulfur tracer wire was fed to the meniscus in the mold. The wire was melted by the nozzle discharge stream, and the tracer was carried deep into the pool by the downward flow. When a 0.55 T magnetic field was applied, the penetration depth of the tracer was approximately halved as compared with the case when no electromagnetic braking was applied (see **Fig. 14**). This result shows the effect of electromagnetic braking in preventing the inclusions and bubbles introduced into the mold pool through the immersion nozzle from penetrating deep into the pool. When the change of mold meniscus temperature with electromagnetic braking was investigated, a temperature rise of about 10°C was observed as compared with the case in which no electromagnetic braking was applied. This phenomenon can be explained also by the decrease of penetration depth by electromagnetic braking.

3.2.2 Suppression of mixing

The casting conditions of **Table 2**(b) concern the experiment in which an iron-covered tracer wire designed to melt just below the in-mold electromagnetic brake was added to the pool. When the magnetic flux density was 0 T, the mixing of the melt proceed-

Table 2 Continuous casting conditions for medium-carbon steel with level magnetic field brake

	(a) Tracer added to upper pool	(b) Tracer added to lower pool
Steel grade	Medium-carbon aluminum-silicon-killed steel	Medium-carbon aluminum-silicon-killed steel
Tracer	Sulfur	Sulfur and phosphorus
Casting temperature	1,540°C	1,530-1,560°C
Casting speed	0.5 m/min	0.5 m/min
Mold shape	600 mm wide × 100 mm thick	600 mm wide × 100 mm thick
Meniscus-to-core distance	920 mm	920 mm
Maximum magnetic flux density	0.55 T	0.55 T

ed throughout the pool, and the molten tracer was dispersed and mixed with the molten steel by the nozzle discharge stream and reached the upper pool. As a result, the tracer was distributed throughout the transverse section of the slab as shown in **Fig. 15**(a). When a 0.55 T magnetic field was applied, the lower pool in which the tracer was melted and mixed with the molten steel was separated by the level magnetic field brake from the upper pool. The tracer did not diffuse into the upper pool, either. When the transverse section of the cast slab was examined, the tracer distribution was confined to the core of the slab, as shown in **Fig. 15**(b). Also, as shown in **Fig. 16** (b), the tracer concentration steeply rose in the core of the slab. These results clearly indicate that the molten steel in the upper pool is prevented from mixing with that in the lower pool by braking with a level magnetic field.

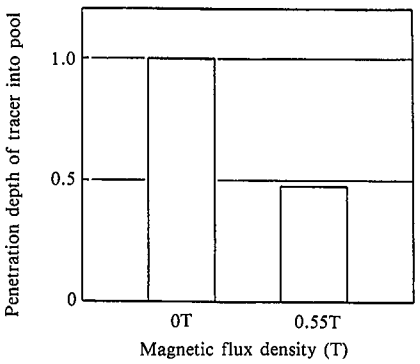

Fig. 14 Change in penetration depth of tracer into pool with level magnetic field braking

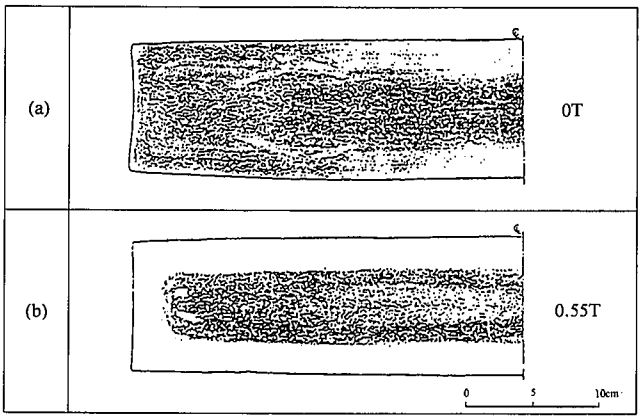

Fig. 15 Distribution of tracer (sulfur) added to pool on cross section of cast slab

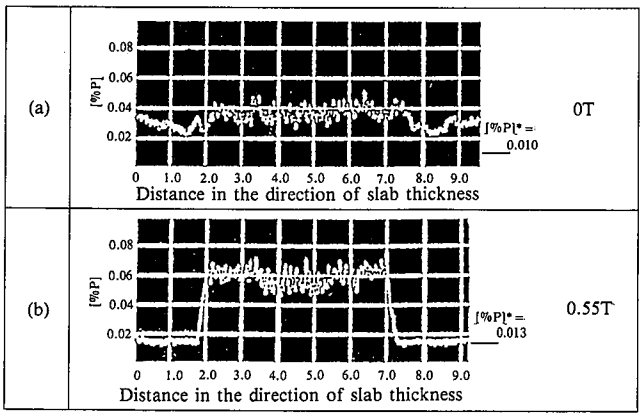

Fig. 16 Concentration distribution of tracer (phosphorus) added to pool in thickness direction of cast slab

4. Control of Initial Solidification by Electromagnetic Pressure

The surface of a continuous cast slab is characterized by oscillation marks. The oscillation marks are considered to result from the reciprocal motion of the oscillating mold and the solidifying shell being withdrawn through the layer of mold flux that flows as lubricant between the mold wall and the solidifying shell. These marks are a troublesome obstacle to improving the surface quality of continuously cast steel. In their basic research on the behavior of molten metal in an alternating-current (AC) magnetic field, the authors clarified that the free surface profile of the liquid metal and the static pressure near the meniscus can be controlled by electromagnetic pressure[10]. This phenomenon can be utilized to control the initial solidification of steel being continuously cast. In other words, electromagnetic force is used to control the meniscus shape and the mold flux channel shape, to relax the dynamic pressure produced in the channel by the mold oscillation, and to stabilize the mold lubrication, thereby improving the steel surface quality.

4.1 Results of plant test

The experimental apparatus is schematically as illustrated in **Fig. 17**. A solenoid coil is installed in the mold water cooling box. The experimental casting conditions are given in **Table 3**[11].

Photo 1 shows bloom surface appearance and subsurface structure when the electromagnetic force was not applied (a) and was applied (b), respectively, during the continuous casting of nickel stainless steel on a bloom caster. When no electromagnetic force was imposed, periodic oscillation marks were formed on the bloom surface as shown in **Photo 1**(a), and typical positive

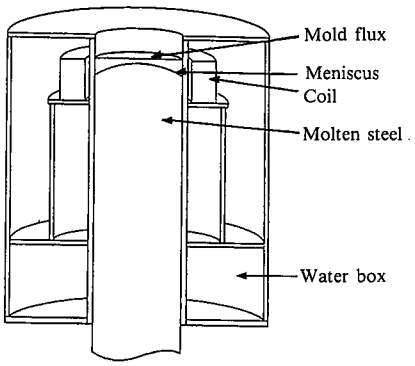

Fig. 17 Schematic illustration of apparatus for controlling initial solidification of molten steel by electromagnetic force

Table 3 Experimental conditions for initial solidification control by electromagnetic force during continuous casting of stainless steel

Steel grade	18-8 stainless steel
Casting temperature	1,495-1,518°C
Casting speed	0.8-1.6 m/min
Mold shape	190 mmϕ
Meniscus-to-core distance	0±10 mm
Maximum magnetic flux density	0.162 T

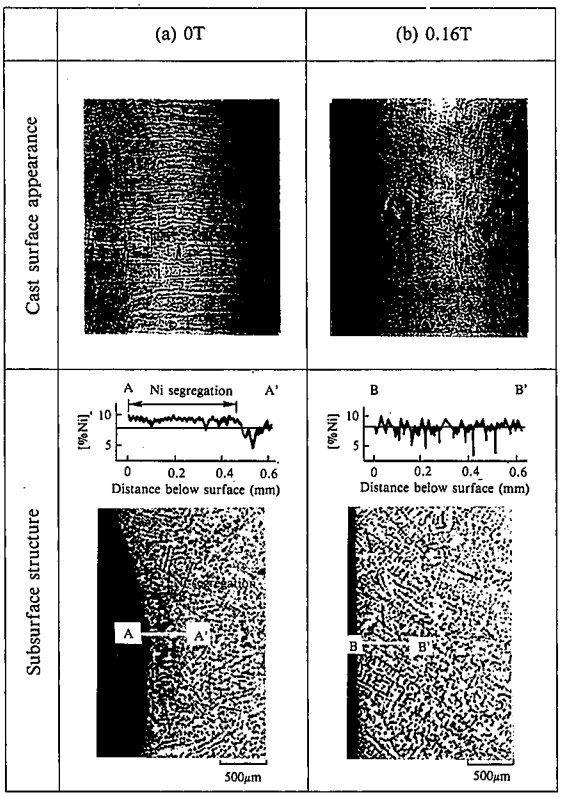

Photo 1 Control of initial solidification by electromagnetic pressure during continuous casting of stainless steel: (a) Cast surface appearance and subsurface structure without electromagnetic force; and (b) Cast surface appearance and subsurface structure with electromagnetic force

nickel segregation was observed in the subsurface layer. The oscillation mark depth decreased with increasing magnetic flux density of the electromagnetic force applied. The bloom surface became virtually smooth when the magnetic flux density was about 0.15 T (see **Fig. 18**). As the oscillation mark depth was reduced, the nickel segregation at the bottom of the oscillation mark was also reduced, and disappeared when the magnetic flux density was increased to about 0.1 T.

4.2 Mechanism of initial solidification control

The meniscus shape is calculated from the balance between the electromagnetic force acting on the molten steel pool and the ferrostatic pressure of the molten steel. The velocity distribution of the molten steel in the pool is also obtained. Then, the temperature distribution in the pool is determined by coupled steady-state analysis of heat transfer and fluid flow by the finite difference method[12].

$$\rho C\frac{\partial T}{\partial t}(h_\xi h_\eta T)=\frac{1}{r}\frac{\partial}{\partial r}(\lambda r\frac{h_\eta}{h_\xi}\frac{\partial T}{\partial r})+\frac{1}{r}\frac{\partial}{\partial z}(\lambda r\frac{h_\eta}{h_\xi}\frac{\partial T}{\partial z}) \quad \cdots\cdots(8)$$

Using Eqs. (9) to (11), the flux flow into the gap between the solidifying shell and mold wall is calculated, and the dynamic pressure of the flux channel is evaluated[13].

$$Q=\{\rho_f g l_f-\Delta P+6\mu_f\Delta v\varepsilon(l_f)\}/\{12\mu_f\zeta(l_f)\} \quad \cdots\cdots(9)$$

$$P_d=P_o+\rho_f g x+6\mu_f\Delta v\varepsilon(x)-\{\rho_f g l_f-\Delta P+6\mu_f\Delta v\varepsilon(l_f)\}\zeta(x)/\zeta(l_f) \quad \cdots\cdots(10)$$

$$\varepsilon(x)=\int_0^{l_f}\{1/J^2(x)\}dx,\quad \zeta(l_f)=\int_0^{l_f}\{1/J^3(x)\}dx \quad \cdots\cdots(11)$$

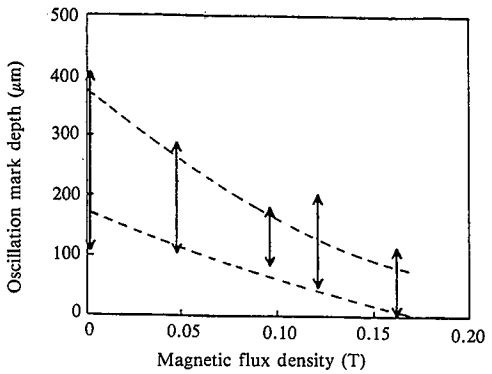

Fig. 18 Reduction in oscillation mark depth with increasing magnetic flux density

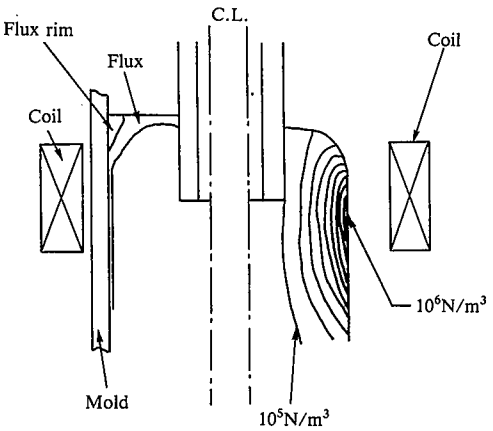

Fig. 19 Change in static pressure distribution in pool with AC magnetic field application

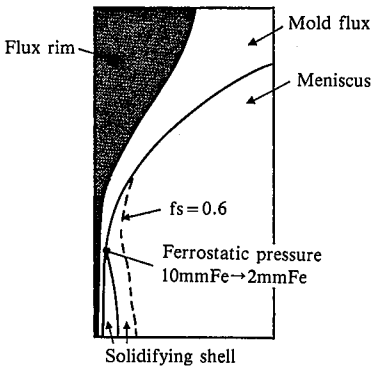

Fig. 20 Temperature distribution in initial solidification region with electromagnetic pressure

Fig. 19 shows the distribution of static pressure brought about by the electromagnetic pressure generated in the molten steel pool in the mold. The meniscus becomes convex, and the static pressure acting on the solidifying shell is diminished. The amount of heat generated in the molten steel by electromagnetic induction is almost ignorable compared with the amount of heat extracted.

Fig. 20 shows the temperature distribution in the region where the molten steel solidifies first. The electromagnetic force causes the meniscus to form a convex shape. The change of temperature distribution with the expansion of the flux region allows the

growth of the flux rim right above the top of the solidifying shell. When compared with the case in which no electromagnetic force is applied, the flux channel thickness is increased, and the dynamic pressure acting on the top of the solidifying shell is decreased.

The decrease in the depth of oscillation marks formed on the bloom surface can be explained in this way. The increase of resistance to heat extraction with the increase of flux channel thickness decreases heat extraction at the meniscus to set back the starting point of shell solidification. This is also considered a factor in the smoothing of the bloom surface.

5. Conclusions

Application of MHD in the continuous casting process started with the electromagnetic stirring of stand pool with a traveling magnetic field. It has now advanced to the electromagnetic stirring of molten steel in the mold and the control of molten steel flow by an in-mold DC magnetic field brake. These applied MHD techniques are designed to further improve the continuous casting process capability. They improve the surface quality of cast steel by homogenizing the meniscus temperature, stabilizing initial solidification and cleaning the surface layer. They also improve the internal quality of cast steel by preventing inclusions from penetrating deep into the pool and promoting the flotation of argon bubbles.

Applied MHD technology is advancing in scope and methods in addition to molten steel stirring and braking. Among such advances are: 1) suppression of CO blowhole formation by controlling reaction at the solidification front; 2) casting of bimetallic slab by suppressing mixing in the pool; and 3) control of initial solidification by electromagnetic pressure.

Nomenclature

$\mathbb{B}$: Magnetic flux density (T)
C : Specific heat (J/kg·K)
$\mathbb{E}$: Electric field (V/m)
g : Gravitational acceleration (m/s^2)
h_η : Relative scale function in axial direction of pool
h_ξ : Relative scale function in radial direction of pool
J : Shape function of flux channel
$\mathbb{J}$: Induced current density (A/m^2)
P_O : Pressure at inlet side of flux channel (Pa)
P_d : Dynamic pressure in flux channel (Pa)
Q : Relative consumption of flux (m^3/s)
r : Radius of mold pool (m)
T : Temperature (K)
t : Time (s)
$\mathbb{U}$: Velocity (m/s)
ΔV : Velocity difference between mold and solidifying shell (m/s)
x : Distance in casting direction (m)
λ : Thermal conductivity (W/m·K)
μ : Magnetic permeability (H/m)
μ_f : Viscosity of flux (Pa·s)
ν : Kinematic viscosity of liquid metal (m^2/s)
ρ : Density of liquid metal (kg/m^3)
σ : Electric conductivity of liquid metal (S/m)
ϕ : Electric potential (V)

References

1) Takeuchi, E. et al.: Tetsu-to-Hagané. 65 (14), 1615 (1983)
2) Hughes, W.F. et al.: The Electromagnetohydrodynamics of Fluids. New York, John Wiley & Sons, 1966, p. 148
3) Suzuki, S. et al.: CAMP-ISIJ. 5, 188 (1992)
4) Yuyama, H. et al.: CAMP-ISIJ. 1, 1220 (1988)
5) Nagai, J. et al.: Iron and Steel Engineer. 61, 41 (1984)
6) Takeuchi, E. et al.: Magnetohydrodynamics in Process Metallurgy. TMS, 1992, p. 261
7) Zeze, M. et al.: Steelmaking Conference Proceedings. Vol. 76, Dallas, March 1993, ISS-AIME, p. 267
8) Takeuchi, E. et al.: CAMP-ISIJ. 4, 24 (1991)
9) Yoneyama, Y. et al.: Seitetsu Kenkyu. (335), 26 (1989)
10) Miyoshino, I. et al.: ISIJ International. 29, 1040 (1989)
11) Takeuchi, E. et al.: CAMP-ISIJ. 6, 1125 (1993)
12) Toh, T. et al.: CAMP-ISIJ. 6, 1126 (1993)
13) Takeuchi, E. et al.: Metallurgical Transactions B. 15B, 493 (1984)